New evidence for the origin of the Porcupine Median Volcanic Ridge: Early Cretaceous volcanism in the Porcupine Basin, Atlantic margin of Ireland

Gérôme Calvès, Taija Torvela, Mads Huuse, Menno G. Dinkleman

Geochemistry Geophysics Geosystems G3

Article
Volume 13, Number 6
1 June 2012
Q06001, doi:10.1029/2011GC003852
ISSN: 1525-2027

Published by AGU and the Geochemical Society

New evidence for the origin of the Porcupine Median Volcanic Ridge: Early Cretaceous volcanism in the Porcupine Basin, Atlantic margin of Ireland

Gérôme Calvès
GET, Université de Toulouse, UPS (OMP), CNRS, IRD, 14 avenue Edouard Belin, F-31400 Toulouse, France (gerome.calves@get.obs-mip.fr)

School of Earth, Atmospheric, and Environmental Sciences, University of Manchester, Manchester M13 9PL, UK

Taija Torvela
Department of Geology and Petroleum Geology, University of Aberdeen, Aberdeen AB24 3UE, UK

Now at Department of Geosciences and Geography, University of Helsinki, FI-00014 Helsinki, Finland

Mads Huuse
School of Earth, Atmospheric, and Environmental Sciences, University of Manchester, Manchester M13 9PL, UK

Menno G. Dinkelman
BasinSPAN Program, ION-GeoVentures, Houston, Texas 77042, USA

[1] Two-dimensional pre-stack depth migrated seismic reflection data, gravity and velocity models are used to assess the nature and origin of a prominent, buried ridge, the Porcupine Median Volcanic Ridge (PMVR) within the Porcupine Basin, offshore Ireland. The debate on the origin of the PMVR during the past 30 years has followed the evolution of the concept of continental margin genesis. In this paper, the origin of the ridge is evaluated on the basis of the internal geometry and velocity structure, revealed by the seismic data. Implication of the presence of these type of ridges in hyper-extensional rifted margins is discussed and compared with other margins. The analysis indicates that the ridge is an extrusive volcanic ridge, probably tholeiitic in composition, constructed by stacked hyaloclastite deltas and topped by carbonate platforms. The results invalidate previously proposed models involving highly rotated fault blocks and the serpentinite mud volcanism. The extension magnitude analysis suggests a highly stretched setting where limited mantle serpentinization may have occurred, but the architecture and velocity of the PMVR demonstrates that it is made of lower velocity materials than serpentinite. During the opening of the North Atlantic, the PMVR represents the northern time-equivalent magmatic event expressed along the Newfoundland-Iberia-Galicia, recorded by the J anomaly that originate from Cretaceous volcanic deposits.

Components: 9600 words, 12 figures, 1 table.

Keywords: highly stretched continental margin; rift intrabasement high; seismic reflection data; volcanostratigraphy.

Index Terms: 8038 Structural Geology: Regional crustal structure; 8105 Tectonophysics: Continental margins: divergent (1212, 8124); 8169 Tectonophysics: Sedimentary basin processes.

Received 29 August 2011; **Revised** 20 April 2012; **Accepted** 23 April 2012; **Published** 1 June 2012.

Calvès, G., T. Torvela, M. Huuse, and M. G. Dinkelman (2012), New evidence for the origin of the Porcupine Median Volcanic Ridge: Early Cretaceous volcanism in the Porcupine Basin, Atlantic margin of Ireland, *Geochem. Geophys. Geosyst.*, *13*, Q06001, doi:10.1029/2011GC003852.

1. Introduction

[2] Jurassic to Cretaceous rifting of the Atlantic margins from Newfoundland, Goban Spur and Iberia-Galicia, leading to accretion and spreading of oceanic crust, has been documented by various potential field data analyses with challenges on the best fit organization of the different plates, gaps and overlaps (Figure 1a) [e.g., *Sullivan*, 1983; *Srivastava et al.*, 2000; *Sibuet et al.*, 2007]. The conjugated margins of Newfoundland and Iberia-Galicia have been documented by subsurface imagery and sampling, in order to define models for the evolution of non-volcanic rifted margins and hyper-extensional settings and associated upper mantle serpentinitization [e.g., *Boillot et al.*, 1980; *Ranero and Pérez-Gussinyé*, 2010, and references therein]. Recent works on the characterization of magnetic anomalies (Figures 1 and 2, J anomaly, aged ~130–125 Ma [*Bronner et al.*, 2011]) in the conjugate Newfoundland and Iberia-Galicia margins show a potential magmatic event that may have triggered the break-up earlier than the main oceanization pulse in the region. The northernmost extent of this event is, however, not known.

[3] The Porcupine Basin occupies a specific position in the geodynamical evolution of the opening of the North Atlantic (Figure 1). The basin is located north of the rifting event between Iberia and North America, along the propagating rift axis [*Peron-Pinvidic and Manatschal*, 2010]. The basin is situated within the transition between magma-poor continental margins in the south and the magma-rich continental margins in the north. Therefore, the basin is a key element for understanding the transition between magma-poor and magma-rich margin settings, and for understanding the evolution of the opening of the northern Atlantic Ocean. The conclusions of the behavior of highly extended crust and basin evolution in transitional settings are largely dependent on whether or not magmatism occurred. An elongate feature within the basin, buried beneath post-Albian (Early Cretaceous) sediments, has previously been identified as a magmatic ridge, the Porcupine Median Volcanic Ridge (PMVR) [*Tate and Dobson*, 1988]. However, over the last decade this interpretation has been challenged, and the ridge has variously been interpreted as a serpentinite-mud diapir [*Reston et al.*, 2001] or a severely rotated fault block [*O'Sullivan et al.*, 2010a].

[4] The aim of this study is to first test previous interpretations of the PMVR by using high-quality pre-stack depth migrated (PSDM) seismic reflection data from the Porcupine Basin, and second to discuss the implications of this new synthesis on the genesis of this basin. We will (1) re-evaluate the stratigraphic framework and the crustal structure of the basin, (2) document the geophysical characteristics of the PMVR structure, (3) compare seismic images from the PMVR with analogues from other margins, (4) discuss the crustal extension of the basin, estimate the volume of the ridge and its potential life span, and (5) discuss the role of intrabasement highs in rift basin within the break-up to oceanization history of rifted basins. The results demonstrate that the initial interpretation of the PMVR as a dominantly magmatic feature [e.g., *Tate and Dobson*, 1988] remains the most likely explanation. The implications of the results on the relationship between the phased emplacement of the PMVR and the magmatic pulse further south along the J-Anomaly could help to understand the geodynamic evolution of the North Atlantic.

2. Geological Setting

[5] The Porcupine Basin (Figure 1) formed during multiple subsidence and rifting episodes between Late Carboniferous and Late Cretaceous (Figure 2). The pre-Jurassic rifting episode(s), which were minor and resulted in limited crustal thinning, are poorly constrained: in the Triassic, a sequence of multiple minor rifting episodes commenced [*Shannon*, 1991; *Tate*, 1993; *McCann et al.*, 1995; *Doré et al.*, 1999] (Figure 2). This initial rifting period was followed by the main rifting episode in the Middle to Late Jurassic that has been estimated to have lasted for 20–30 Myr, possibly continuing into the earliest Cretaceous (Figure 2). The main rifting was followed by a period of major thermal subsidence, although some authors suggest a period of thermal

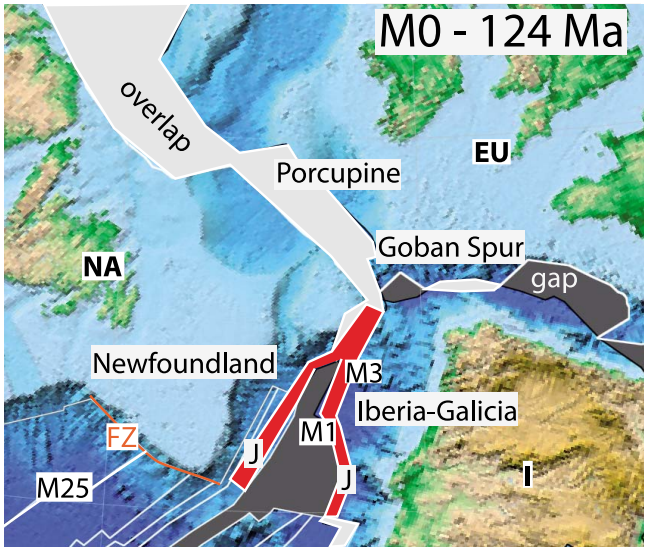

Figure 1. Reconstruction of North Atlantic between North America (NA), Iberia (I) and Eurasia (EU) at chron M0 (~124 Ma). Plate reconstruction established from GPLATES 1.1.1 (www.gplates.org) and associated files (accessed 12/2011). For geomagnetic polarity age M25, M0, M3 and J anomaly see Figure 2. FZ, fault zone. Note the position of the Porcupine Basin and distance from the rifting and drifting between Newfoundland and Iberia-Galicia margins.

uplift after the Jurassic rifting (Figure 2). The period of thermal subsidence was followed by another minor rifting period in the Early Cretaceous (Figure 2). Finally, *Hall and White* [1994] note the presence of Tertiary (Palaeogene) anomalous subsidence in the northern Porcupine Basin and suggest an episode of minor lithospheric stretching caused by rifting or a mantle plume.

[6] The lithosphere of the Porcupine Basin has experienced extreme stretching, especially in the southern parts of the basin as a result of a clockwise rotation of the Porcupine Ridge away from the Irish Shelf by some 20 to 25° (Figures 3a and 3b) [e.g., *White et al.*, 1992; *Tate*, 1993]. The crustal thickness in the South Porcupine Basin has been estimated using various geophysical techniques to 7.5 ± 2.5 km [e.g., *Masson and Miles*, 1986; *Masson et al.*, 1998; *Conroy and Brock*, 1989; *Grad et al.*, 2009; this paper]. Lithospheric stretching in this part of the basin has been estimated to $\beta > 6$ ($\beta = Z_0/Z_1$, with Z_1 the estimated crustal thickness and Z_0 the initial crustal thickness) (Figure 3b) [*White et al.*, 1992; *Tate*, 1993]. The normal faulting interpreted in the basin cannot account for the amount of crustal stretching [e.g., *Baxter et al.*, 2001], but the discrepancy may be explained by depth-dependent lithospheric extension where some of the extension is accommodated by a ductile behavior of the lower crust at the early stages of the rifting (pure shear), with a sub-horizontal detachment developing between the ductile lower crust and the brittle upper crust (simple shear) [e.g., *Reston et al.*, 2004; *O'Reilly et al.*, 2006].

[7] An elongate feature (Figure 3c), buried beneath post-Albian (Early Cretaceous) sediments (Figure 4a) has been identified as a magmatic ridge, the Porcupine Median Volcanic Ridge (PMVR), by *Tate and Dobson* [1988]. The PMVR is Early Cretaceous in age, i.e., late- to post-rift [e.g., *White et al.*, 1992]. There are also at least two other, smaller ridges close to the western margin of the basin (Figure 3c). The ridges have not been drilled, but drilling from the nearby Goban Spur Basin - Western Approaches Margin (Figure 1) has revealed evidence of Valanginian (Early Cretaceous) volcanism with a syn-rift geochemical signature [*Tate*, 1993]. *Reston et al.* [2001, 2004] re-named the ridge as 'the Porcupine Median High', interpreting it as a serpentinite-mud volcano or diapir (Figure 4b). The interpretation was made on the basis of the stretching factor, rift duration, the younger age of the ridge compared to the age of the rifting, and theoretical considerations of the spatial relationship of the ridge with tilted fault blocks and a sub-horizontal detachment (P in Figure 4b). The latest interpretation, by *O'Sullivan et al.* [2010a, 2010b], presents an integrated study of the basin, ruling out a volcanic or metamorphic origin of the ridge. The authors instead interpret the ridge as a severely rotated, crustal fault block

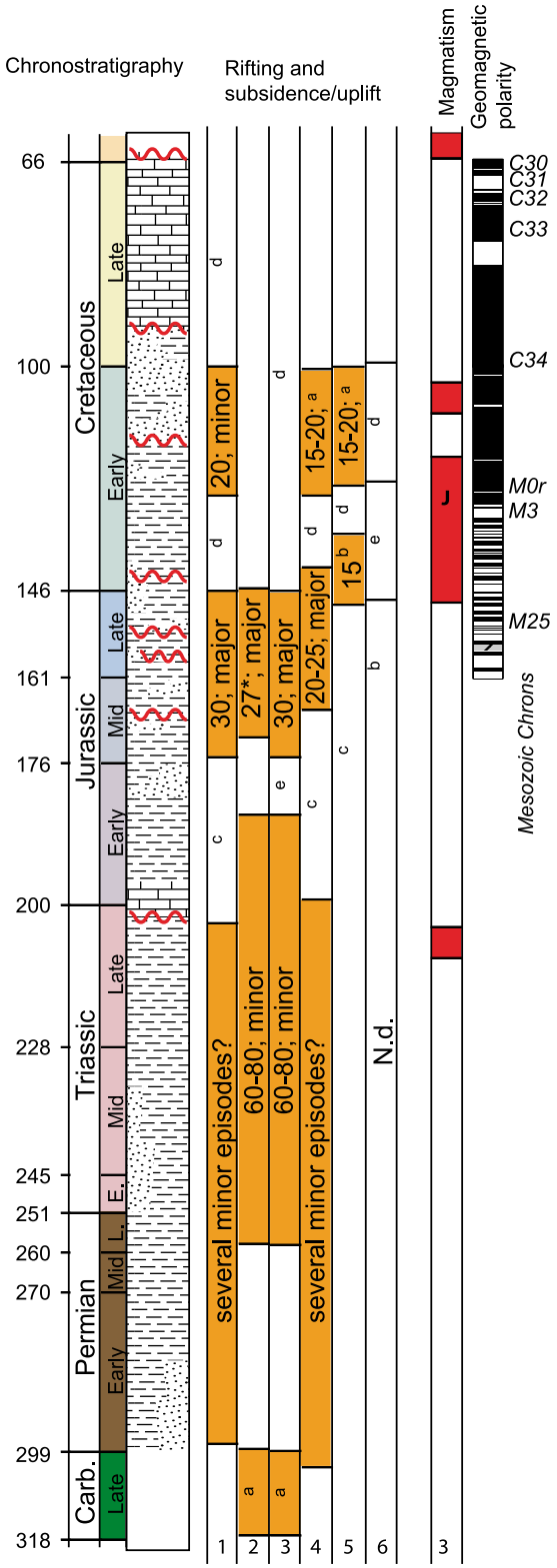

related to hyperextension of the crust, naming it 'the Porcupine Median Ridge' (Figure 4c).

3. Materials and Methods

3.1. Seismic Reflection Data

[8] The approximately 1,500 km of seismic reflection data used in this study are part of the much larger regional NE Atlantic SPAN™ survey acquired and processed by ION GX Technology in 2007–2008. The acquisition was designed for crustal-scale imaging by using a long receiver cable with a 10.2 km maximum offset and a large source size of 7,440 cu inch with 253 barm peak output. The air gun and the geophones were towed at depths of 17.5 m and 18 m, respectively, keeping the bubble interference to a minimum. The air gun and streamer deep-tow provided a maximum energy input at 20–30 Hz frequency, allowing the acoustic penetration of basaltic intervals known to cause significant acoustic attenuation. Crustal-scale imaging is achieved by an 18 s two-way time record (or 40 km depths). The prestack depth-migrated data were migrated (Kirchhoff PSDM) using velocities derived from iterative tomographic velocity modeling [e.g., *Deregowski*, 1990]. The modeled depths are within 5% of the depths from calibration wells. The profile locations are shown in Figure 3a.

3.2. Other Geophysical Data

[9] A free-air gravity anomaly model based on the global compilation by *Sandwell and Smith* [2009] was included in the database available for the project (Figure 3c). Potential field data and seismic refraction data were used to study the crustal geometry of the Porcupine Basin and the surrounding area.

Figure 2. Chronostratigraphy and tectonic, magmatic episodes in the Porcupine Basin according to the literature and geomagnetic polarity from late Jurassic to late Cretaceous. The stratigraphic column is from *Shannon* [1991]. The (maximum) duration of each rifting episode (Myr) is indicated, if given by the author(s). Note that *Tate et al.* [1993] suggest that the rifting started in the Early Bajocian, the age of which has been redefined from c. 180 Ma to c. 172 Ma, reducing the estimated rift duration from 35 to 40 Myr to a maximum of 28 Myr. 1, *Shannon* [1991]; 2, *Tate et al.* [1993]; 3, *Tate* [1993]; 4, *McCann et al.* [1995]; 5, *Williams et al.* [1999]; 6, *Jones et al.* [2001]; a, minor rifting; b, major rifting; c, minor thermal subsidence; d, major thermal subsidence; e, thermal uplift; asterisk, corrected rift duration (from Early Bajocian to end of Tithonian, as interpreted by *Tate et al.* [1993]) from 35 to 40 Myr to c. 27 Myr. N.d = not discussed.

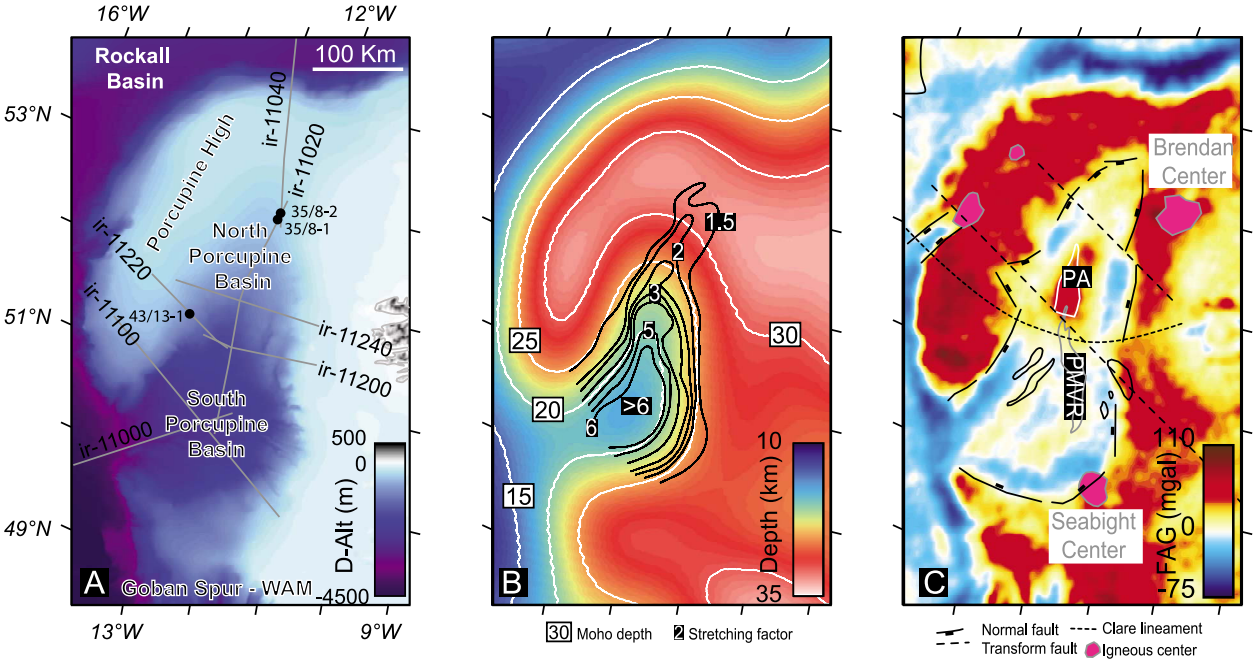

Figure 3. Setting of the Porcupine Basin (North Porcupine Basin and South Porcupine Basin). (a) Seafloor bathymetry from GEBCO compilation (https://www.bodc.ac.uk/data/online_delivery/gebco/; *British Oceanographic Data Centre*, 2003), pre-stack depth migration (PSDM) seismic reflection survey in light gray: NE Atlantic SPAN© (ION-GXT®), boreholes are indicated by the filled black circles. (b) Average Moho depth map from the European Seismological Commission–Working Group "Crustal Structural Maps of Europe" (http://www.seismo.helsinki.fi/mohomap/) [*Grad et al.*, 2009]. Beta factor estimates are overlain as black contours [*Tate et al.*, 1993]. (c) Free-air gravity anomaly map of the area (V18, http://topex.ucsd.edu/cgi-bin/get_data.cgi) [*Sandwell and Smith*, 2009] and the main structural features, including the PMVR and the two smaller ridges to the west of the PMVR [*Tate*, 1993]. The normal faults and igneous centers from Petroleum Affairs Divisions, DCENR and Government of Ireland (http://gis.dcenr.gov.ie/imf/imf.jsp?site=PAD_Seismic); transform fault from *Readman et al.* [2005], and Clare Lineament from *Bentley and Scrutton* [1987]. PA: Porcupine Arch; PMVR: Porcupine Median Ridge.

The reference Moho depth model used in this study was compiled by the European Seismological Commission [*Grad et al.*, 2009] (Figure 3b). To analyze the crustal affinity of the Porcupine Basin and surrounding area, the PSDM velocity model was compared with the basement velocity profiles from previous studies (Figure S1 in the auxiliary material).[1]

3.3. Tectono-Stratigraphic Framework

[10] The regional interpretation of the 2D seismic reflection data is based on the principles of seismic stratigraphy [*Mitchum et al.*, 1977]. The resulting seismic stratigraphic framework has been calibrated to previous studies (Figure 2) [e.g., *Ziegler*, 1988; *Tate and Dobson*, 1989; *Shannon*, 1991; *Tate*, 1993; *Sinclair et al.*, 1994; *Moore and Shannon*, 1995; *Jones et al.*, 2004] and three boreholes: two in the North Porcupine Basin (35/8–1 and 35/8–2 [*Tate and Dobson*, 1988; *Readman et al.*, 2005] (Figures 3a and 5)), and one on the eastern side of the PMVR (43/13–1 [*Johnston et al.*, 2001] (Figures 3a and 6)). The regional Base Cretaceous Unconformity marks the top of the basement (i.e., the crust/pre-rift sequence) in this study (BCU in Figure 5). Above the BCU lies a Cretaceous to Cenozoic (post-rift) sequence, the upper boundary of which is the seafloor.

3.4. Seismic Volcanostratigraphy

[11] The seismic volcanostratigraphic concept employed here is inherited from *Mitchum et al.* [1977] and is based on seismic stratigraphy and sequence stratigraphy methods developed in the early 1970s on siliciclastic and carbonate sedimentary systems. This method was then applied to the observation and recognition of volcanic or volcanoclastic sedimentary systems along rifted volcanic margins [e.g., *Symonds et al.*, 1998;

[1]Auxiliary materials are available in the HTML. doi:10.1029/2011GC003852.

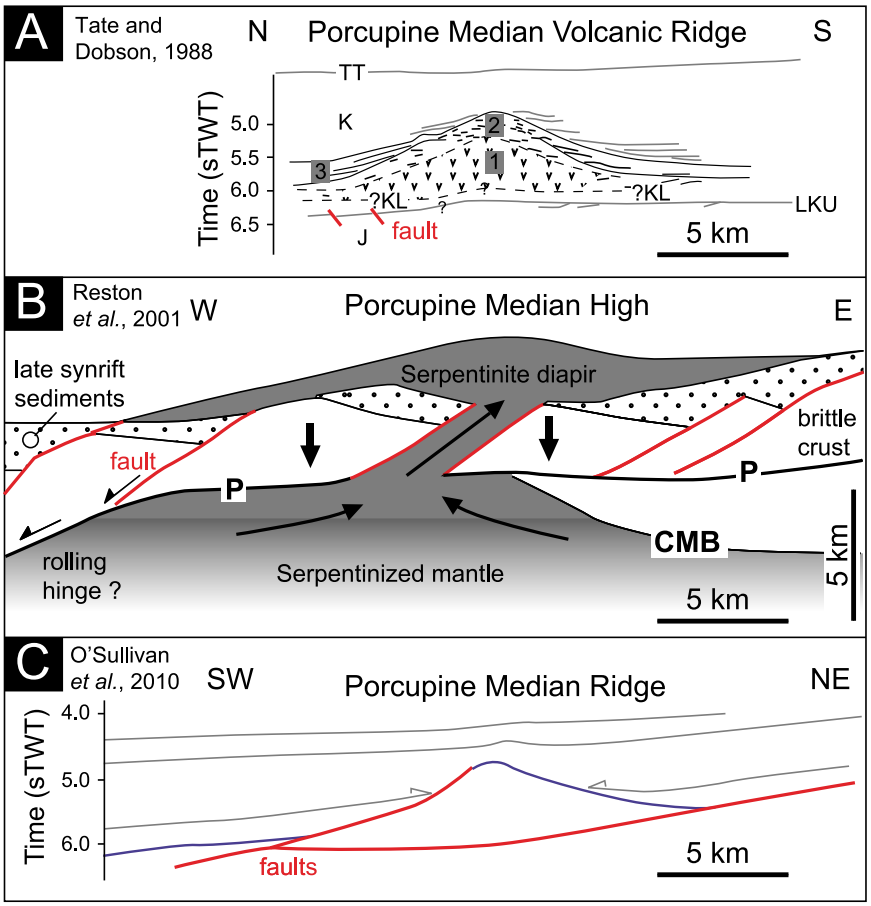

Figure 4. The three suggested origins for the Porcupine Median Volcanic Ridge. (a) Volcanic origin. J, Jurassic; ?KL, Lower Cretaceous; K, Cretaceous undifferentiated; LKU, late Kimmerian unconformity; TT, Tertiary. Layers: 1, homogenized core region of chaotic discontinuous reflections; 2, narrow outer zone surrounding the core with higher amplitude and lower frequency reflections dipping at low angles down the flanks; 3, marginally developed wedge-shaped zone of parallel and continuous reflections inclined at higher angle than layers 1 and 2. (b) "Metamorphic" origin, serpentinite diapir. P, detachment; CMB, crust-mantle boundary. (c) Sedimentary/fault block. Vertical scale varies between the drawings while, the horizontal scale is identical for the three sections. Note the various orientations of the profiles. Figure 4a is adapted from *Tate and Dobson* [1988]; Figure 4b is adapted from *Reston et al.* [2001]; and Figure 4c is adapted from *O'Sullivan et al.* [2010a], AAPG©2012, reprinted by permission of the AAPG whose permission is required for further use.

Kiørboe, 1999; *Planke et al.*, 1999, 2000]. First, the seismic volcanostratigraphic interpretation leads to the identification of a basaltic sequence. Second, identification and interpretation of characteristic internal reflections leads to the definition of volcanic seismic facies units and edifices. Finally, the seismic facies observations are then interpreted in terms of volcanic and sedimentary processes, as shown in previous studies [*Symonds et al.*, 1998; *Planke et al.*, 1999, 2000; *Berndt et al.*, 2001; *Rey et al.*, 2008; *Calvès et al.*, 2011]. The mapping of the seismic facies and reflection stacking patterns differs from the classic scheme of clastic seismic sequence stratigraphy. Concepts such as the non-unique lateral transition of facies, are hard to apply with sparse seismic reflection grids and limited predictive seismic facies correlation calibrated with equivalent active volcanic depositional systems. This will be highlighted in the following sections.

4. Observations

4.1. Potential Field Data

[12] The free-air gravity anomaly data display two main domains: positive values are mainly associated with the Porcupine High, and with the Irish Continental Shelf and Celtic Sea, while negative values are found within the Porcupine Basin itself. Normal faults observed in the subsurface are located

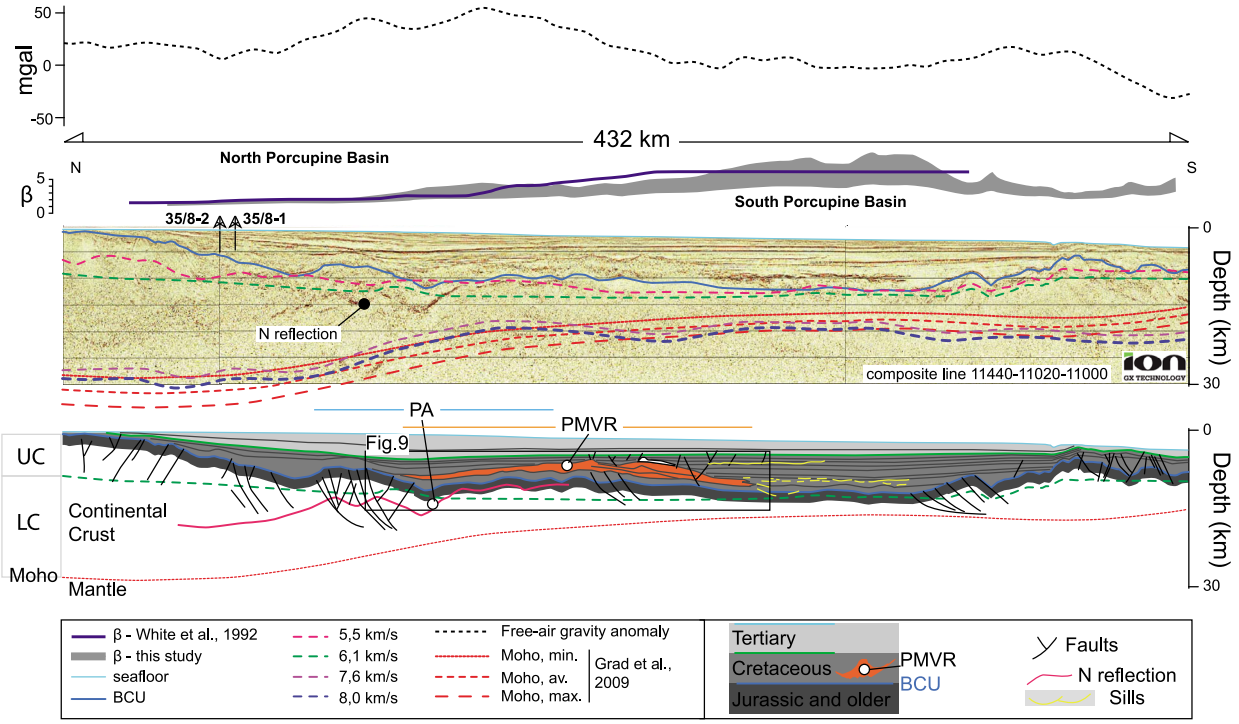

Figure 5. Crustal-scale pre-stack depth-migrated seismic reflection profiles of the Porcupine Basin (uninterpreted and with a line drawing of the main interpreted stratigraphic and structural elements), a composite, N–S seismic reflection profile (see Figure 3a for location). The profiles also show the free-air gravity anomaly [*Sandwell and Smith*, 2009], and the minimum and maximum estimated Moho depths from the European Seismological Commission–Working Group "Crustal Structural Maps of Europe" [*Grad et al.*, 2009]. Borehole locations are plotted above the seismic lines. UC, Upper Crust; LC, Lower Crust; PA, Porcupine Arch.

in the transition between these domains [e.g.: *Tate*, 1993] (Figure 3c). In the center of the basin, two distinctive gravity anomalies are observed along a N-S axis. The northernmost anomaly with high values of 30–56 mgal corresponds to the so-called Porcupine Arch [e.g., *Johnson et al.*, 2001], whereas the southern anomaly with values of 3–24 mgal corresponds to the PMVR (Figures 3c and 6) and the other smaller ridges [*Tate and Dobson*, 1988] (Figure 3c). The Porcupine Arch (PA in Figure 3c) gravity anomaly (high) is spatially associated with a locally increased seismic velocity gradient under the Arch (Figure 5) (seismic refraction experiment RAPIDS 4) [*O'Reilly et al.*, 2006] (Figure S1 in the auxiliary material).

4.2. Seismic Reflection Data

[13] The most important and individual elements recognized in the seismic reflection data are briefly described.

4.2.1. Sub-base Cretaceous Unconformity Features

[14] In the northern part of the Porcupine Basin, a strong reflective event is observed that shallows from the edge of the basin toward its center (N reflection, Figures 5 and 7) [see also *Tate and Dobson*, 1988]. At the basin edges, the N reflection occurs within the middle of the lower continental crust, crossing the boundary to the upper continental crust near the southern tip of the Porcupine Arch. The lateral extent and base of the event was delimited from the seismic data, showing that the event is absent in the southern part of the Porcupine Basin (Figures 5 and 7). Below the BCU, major faulting related to the rifting of the Porcupine Basin is associated with the event. Most notably, the N reflection is cut and offset at the basin margins by steeply dipping faults reaching into the lower crust (Figures 5 and 7). Only minor faulting affects the PMVR or the post-rift sequences (Figure 6).

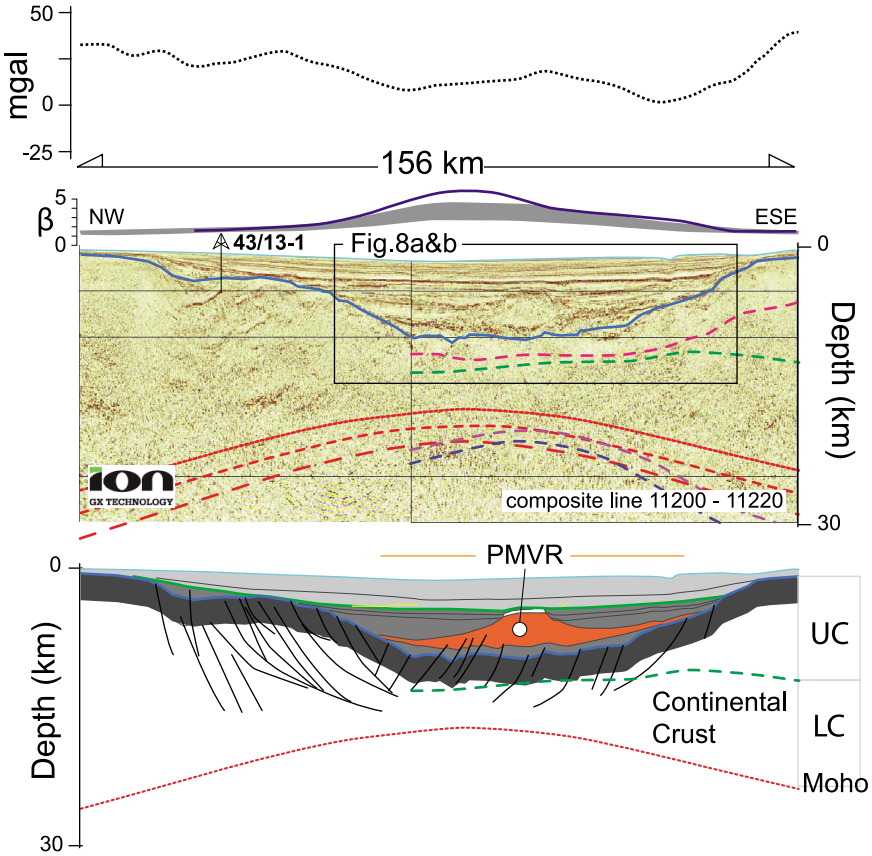

Figure 6. Composite W–E seismic reflection profile across the Porcupine Median Volcanic Ridge (see Figure 3a for location and Figure 5 for legend).

4.2.2. Cretaceous Features

[15] Cretaceous regional markers onlap onto the PMVR (Figures 5–7). The architecture of the PMVR and its P wave velocity structure are outlined in Figures 8–10. The top of the PMVR corresponds to a prominent high amplitude reflection seismic event (Figure 8a), and its base is marked by the transition from low amplitude to high amplitude seismic reflection (Figure 8a). The seismic facies observed within the PMVR are summarized in Table 1 and framed within the seismic volcanostratigraphic framework designed by *Symonds et al.* [1998] and *Planke et al.* [1999, 2000] (inset in Figure 8a). Three main seismic facies correspond (1) to the top of the PMVR associated with landwards flows, (2) the slope of the PMVR where hyaloclastite-lava delta clinoforms prograde away from the vent, and (3) the distal base of the slope of the ridge being inner flows pinching out toward the edge of the Porcupine Basin and BCU surface (Figures 8a and 8c). The internal seismic architecture of the sequence comprises clinoforms with parallel to sub-parallel, gently dipping topsets [*Emery and Myers*, 1996], chaotic reflections in the center of the edifice, and foresets at the edges (Figures 8a and 8b). The pattern of prograding seismic reflection packages observed within the PMVR expresses a divergent direction of progradation. From the geometry and the seismic facies, a volcanic sequence can be defined from bottom to top of the PMVR (Figure 8a).

[16] The ridge is composed of two identifiable mounds (composed of stacked sequences defined by lateral seismic facies: inner flow, hyaloclastite delta and landward flows (Table 1) [*Calvès et al.*, 2011]): 'mound M1' above the BCU, and 'mound M2' on top of M1 (Figure 8c). In the east–west seismic section, the mound shape (M1) of the PMVR is outlined, the thickness of the ridge increasing from the edges of the Porcupine Basin toward its center (Figure 8c). Three sequences have been identified within M1. The basal sequence 1 extends for over 73 km above a faulted sequence with a lower boundary marked by the BCU. The seismic

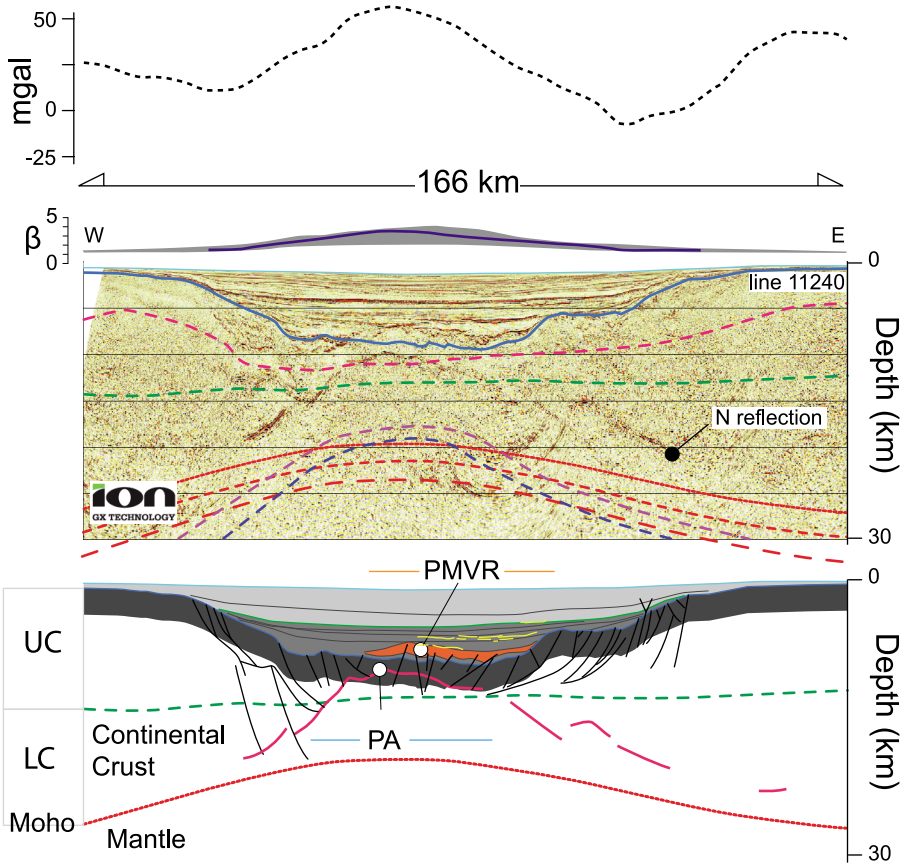

Figure 7. W–E seismic reflection profile 11240 across the Porcupine Arch (see Figure 3a for location and Figure 5 for legend).

reflections within the thin sequence 1 are poorly defined in the center of the ridge but gain continuity toward the edge of the ridge. The thickness of sequence 1 ranges from 100 m at the basin edge, to 1850 m in the center of the basin. The core of the sequence defines an 11 km wide dome-shaped feature. Sequence 2 has a smaller extent of ~50 km from west to east. Its thickness ranges from less than 100 m on its edges, to 1230 m in the center. The seismic reflection patterns are discontinuous and wavy within sequence 2. The shallowest part of the sequence lies above the axis of the dome of sequence 1. Sequence 3 extends ~25 km from west to east and shows a thickness ranging from <100 m to ~1540 m.

[17] The PMVR was flattened on a regional event along the north–south profile in order to restore the basin geometry at the time of the 'drowning' of M2 at the top of ridge. The resulting geometry and the seismic velocity structure of the ridge are outlined in Figures 9 and 10. Along its length, the ridge is composed of two laterally stacked mounds, with mound M2 lying above mound M1 (Figure 9b). All three sequences of M1 are present in the southern part of the ridge where they show progradation toward the south. The progradational unit is associated with P wave velocities ranging between 4 km/s at the top of the ridge and 5.5 km/s at its base (Figures 10a and 10b). Laterally, the velocity slowly decreases from north to south with a high velocity body spatially associated with the Porcupine Arch where the N reflection and a highly faulted crust is imaged (Figure 9b). The ridge itself is composed of a series of lenses of higher velocity that does not, however, exceed 5.5 km/s (Figures 9a and 10a). Toward its southern edge, the ridge thins to an interval of high velocity of >5.5 km/s that is spatially associated with a high amplitude, continuous and wavy reflection package (Figure 10a).

4.3. Crustal Architecture and P Wave Velocity

[18] The seismic reflection data and the velocity model allow a comparison of the Moho depth and

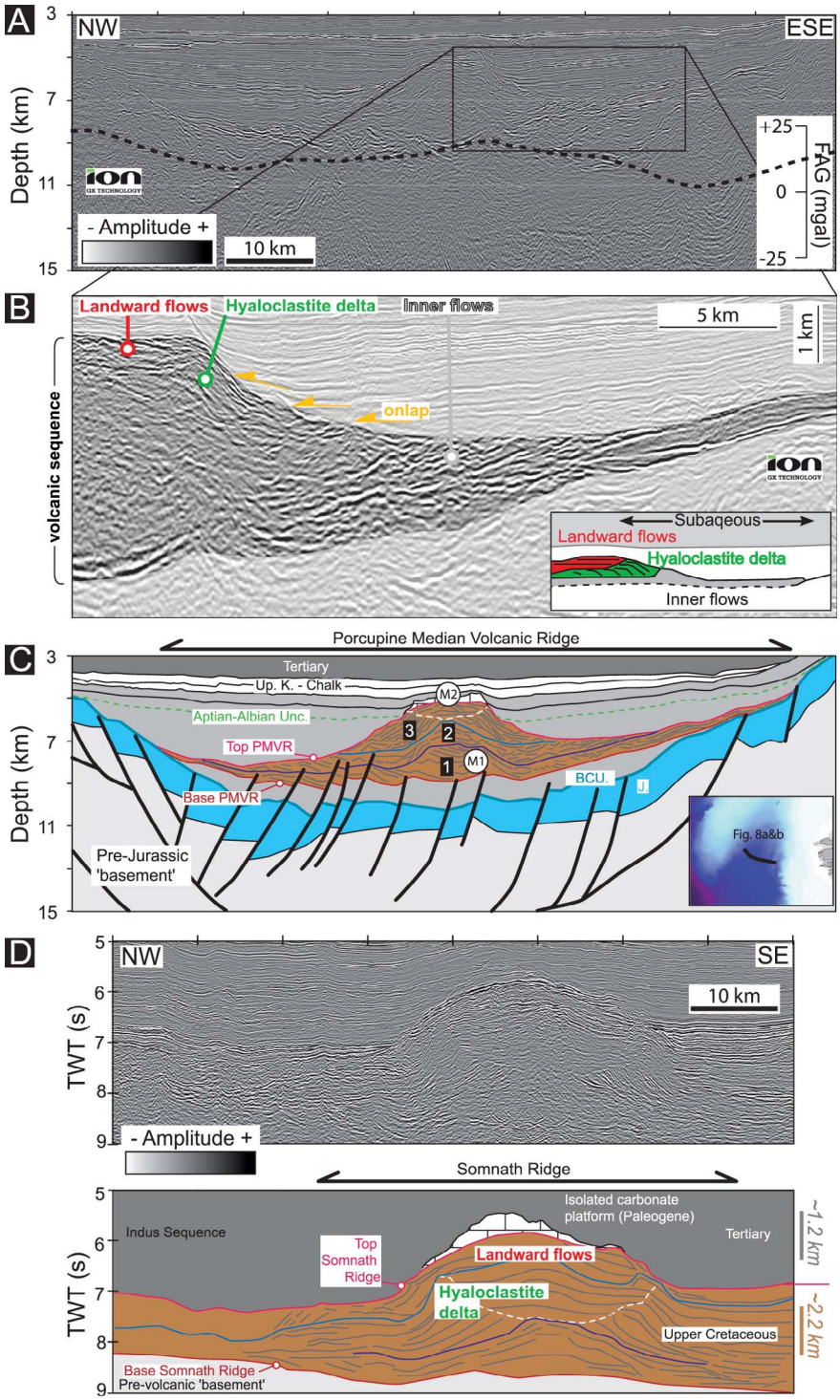

Figure 8. (a) Seismic reflection profile 11200–11220 crossing the PMVR. (b) Detailed seismic reflection profile of the Porcupine Median Volcanic Ridge and associated seismic facies. The inset shows a volcano-stratigraphic facies model adapted from *Symonds et al.* [1998] and *Planke et al.* [1999, 2000]. (c) The PMVR shows prograding seismic reflection packages interpreted as hyaloclastite deltas: sequence 1 is associated with a mound "M1," and sequences 2 and 3 with mound "M2." The offlap break of the hyaloclastic deltas is outlined by the white dashed line within sequence 3. J., Jurassic; BCU, Base Cretaceous Unconformity. (d) An analogue to the PMVR: the Somnath Ridge on the West Indian Margin (offshore Pakistan), vertical scales for the Tertiary and Upper Cretaceous interval are projected along the line drawing for scale comparison. Both ridges show similar prograding seismic reflection packages interpreted as hyaloclastite deltas.

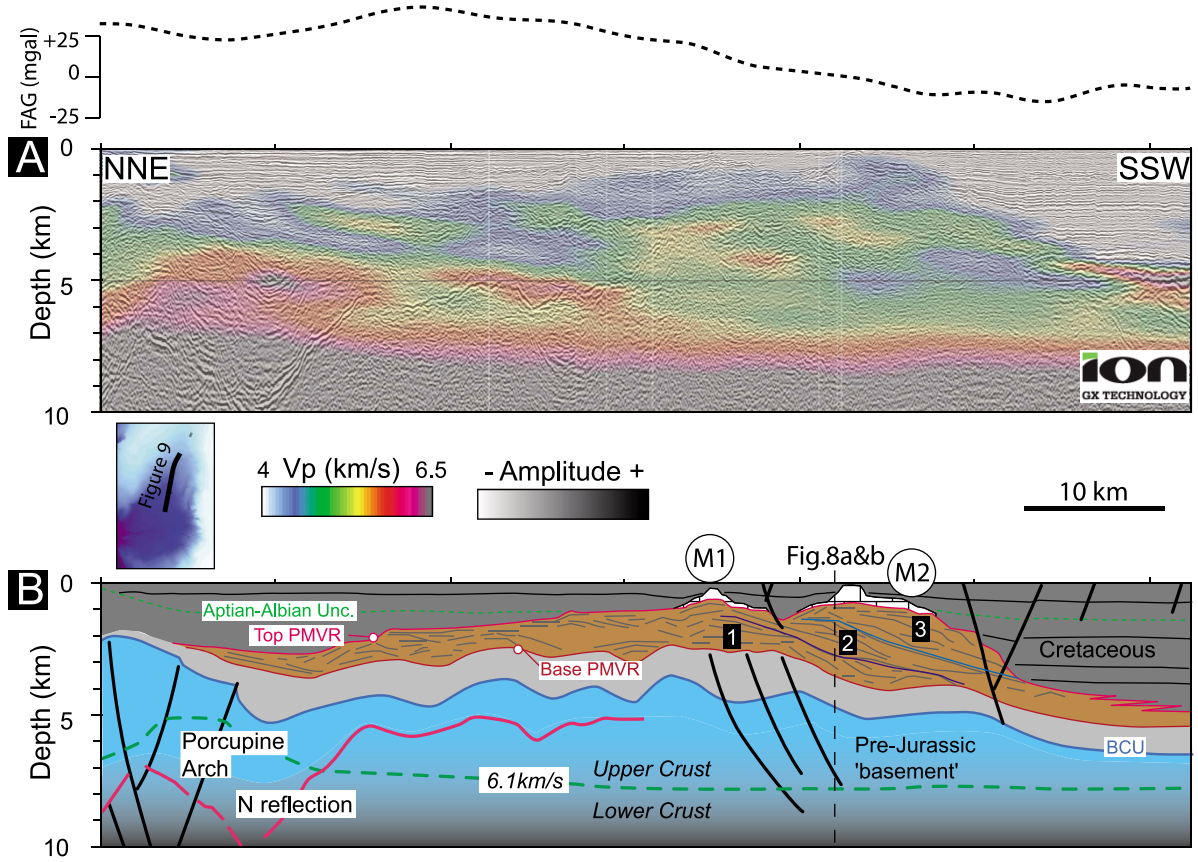

Figure 9. The N–S oriented seismic line along the Porcupine Median Volcanic Ridge (PMVR), flattened along a continuous regional event allowing restoration of the basin geometry at the time of the drowning of the carbonate platform above the ridge. (a) The seismic reflection data overlain with the velocity P wave model (velocity range from 4 to 6.5 km/s). The dashed curve is the free-air gravity anomaly. (b) The corresponding interpreted section. Note the thickened interval of the PMVR made of southward-prograding reflection packages associated with mound M2 (i.e., sequences 2 and 3, see Figures 8a and 8b).

the velocity variations across the study area (see Figure S1 in the auxiliary material). On a north–south profile across the Porcupine Basin (Figure 5), the Moho depth shallows from ~30 km in the north to 15–20 km in the south. The Moho depth in the PSDM velocity model (e.g., 8 km/s in Figure 5) shows a higher degree of short wavelength undulations compared to the regional Moho model [*Grad et al.*, 2009]. This is especially evident below the area where the Porcupine Arch (PA) and PMVR overlap (Figure 5). In the east–west oriented profiles (Figures 6 and 7), the Moho depth shallows from >30 km at the edge of the basin, to 17 km in the center of the basin. The velocity structure reflects the asymmetry of the crust: in the North Porcupine Basin, the slope of the Moho is steeper on the western side of the basin (profile 11240; Figure 7), whereas the inverse is true farther south (profile 11200–11220; Figure 6). *Readman et al.* [2005] suggest that the asymmetry is a result of the transform component in the genesis of this basin (Figure 3c).

5. Discussion

5.1. Model for the N Reflection and the PMVR

[19] The N reflection is present in the upper crust, and is absent in the South Porcupine Basin. It is also cut by late, steeply dipping faults that extend down into the lower crust (Figures 5, 7, and 9). Depth-dependent extension for the basin has been suggested by, e.g., *Baxter et al.* [2001]. Depth-dependent extension necessitates the presence of a gently dipping detachment in the lower and middle crust [e.g., *Johnson et al.*, 2001; *Reston et al.*, 2001, 2004]. Therefore, the N-reflection is, at least partly, likely to follow the detachment that accommodated a large amount of the lithospheric

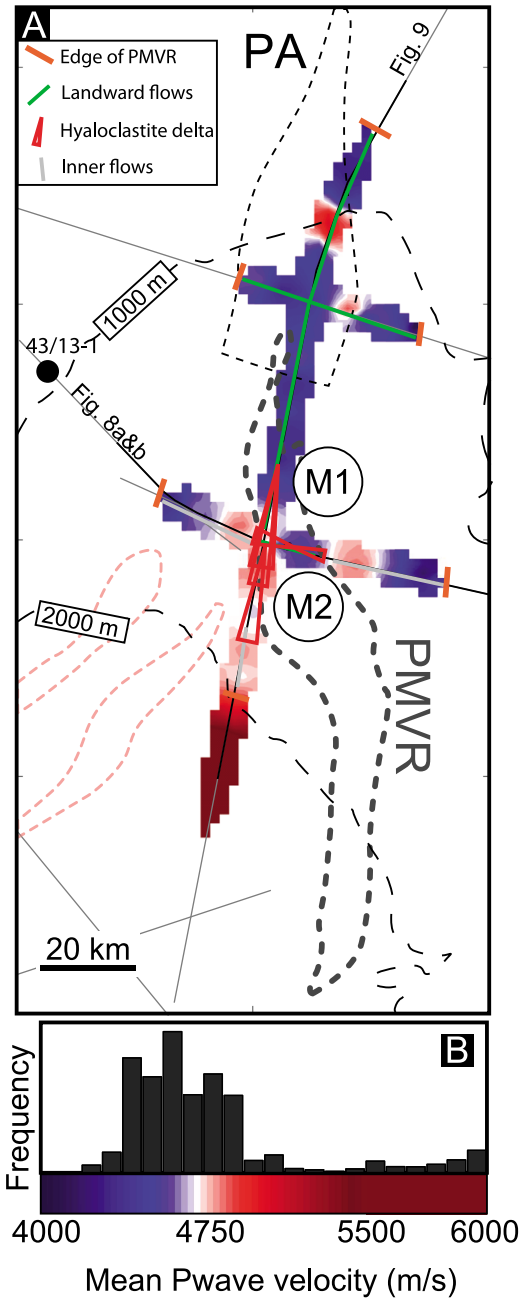

Figure 10. (a) The mean P wave velocity map of the Porcupine Median Volcanic Ridge and seismic facies. (b) The relative frequency histogram extracted from the mean P wave velocity. Note the high-velocity zone in the southern part and the narrow high-velocity zone in the northern part of the ridge. Toward the south, the velocity increases to >5500 m/s. The observed width of the ridge (the orange lines) is larger than previously estimated (light gray dashed lines). The progradational hyaloclastite sequences of mounds M1 and M2 are outlined by the red triangles. The bathymetric contour spacing is 1000 m (black dashed lines). PA, Porcupine Arch; PMVR, Porcupine Median Volcanic Ridge.

stretching. However, the faults crosscutting the reflection indicate that the detachment cannot represent the interface between the lower crust and the mantle as inferred by *Reston et al.* [2001, 2004]. Furthermore, the extent and the geometry of the reflection indicate that other processes than detachment were involved in its formation. In the northern part of the basin, the N-reflection is associated with the gravity anomaly of the Porcupine Arch. The spatial relationship between the gravity anomaly beneath the Porcupine Arch and the high seismic velocity gradient (Figure 5) is interpreted to indicate a presence of melts in the lower crust of the Porcupine Arch. It is, therefore, suggested that the N-reflector contains magmatic rocks originating from the lower crust beneath the Porcupine Arch. The N-reflector may, in other words, represent a magma channel feeding the PMVR. Lateral transport of magmas along and below crustal detachment zones in orthogonal extensional basin settings has been suggested by e.g., *Corti et al.* [2003]. Their results imply that lateral magma transport is facilitated by the lateral flow of ductile lower crust toward the basin center.

[20] Toward its southern edge, the PMVR thins to an interval of high velocity of >5.5 km/s that is spatially associated with a high amplitude, continuous and wavy reflection package (Figures 9a and 10a). The high amplitude, high velocity package is interpreted to represent igneous intrusions associated with the inner flows. *Tate and Dobson* [1988] interpreted the PMVR to be made of extrusive igneous rocks in the south and intrusive rocks to the north from an inferred fissure volcano to a laccolith. Based on our observations, the extrusive component of the ridge is consistent with their interpretation, whereas the presence of a laccolith cannot be confirmed. The mean velocity of the ridge is substantially lower (~4.7 km/s) than the velocity of 5.5 to 6.1 km/s possible for a serpentinite mud volcano [e.g., *Courtier et al.*, 2004].

[21] The three observed seismic reflection patterns of mound M1 within the ridge indicate that the ridge comprises a series of aggrading to prograding depositional elements (clinoforms) evolved during three separate stages (Figure 8c). The interpretation is based on the features that were also recognized on conventional reflection seismic data [*Tate and Dobson*, 1988]. The sequences observed in the PMVR correspond to progradational hyaloclastite deltas previously documented in the North Atlantic and in the Indus Basin [*Planke et al.*, 1999; *Kiørboe*, 1999; *Calvès et al.*, 2011]. The relatively

Table 1. Volcano-Stratigraphic Seismic Facies and Units Associated With the PMVR

	Reflection Boundaries		
Seismic Facies/Unit	Shape/Geometry	Boundaries	Internal
Landward flows	Sheet	Top: high amplitude, smooth. Overlying: onlap or concordant. Base: low amplitude - disrupted.	Parallel to subparellel. High amplitude, disrupted.
Hyaloclastite delta	Bank	Top: high amplitude or reflection truncation. Overlying: onlap or concordant. Base: high amplitude.	Prograding clinoform, disrupted.
Inner flows	Sheet	Top: high amplitude, disrupted. Overlying: conform or onlap. Base: negative amplitude, but often obscured.	Chaotic or disrupted, subparallel.
Hyaloclastite mound	Mound	Top: high amplitude, smooth. Overlying: onlap or concordant. Base: low amplitude, disrupted.	Divergent to subparallel.

low mean velocity together with the overall structure of the ridge implies that the serpentinite diapir model of *Reston et al.* [2001, 2004] can be ruled out. The interpretation of the PMVR being a rotated fault block [*O'Sullivan et al.*, 2010a, 2010b] is also difficult to reconcile by the observations made in this study. Consequently, the original interpretation of the PMVR being an extruded volcanic body [*Tate and Dobson*, 1988] remains the best explanation for the observed features described herein.

5.2. Crustal Extension

[22] The thinning model of *Tate et al.* [1993] with stretching factors of $\beta > 6$ (Figure 3b) was tested by calculating upper crustal thickness estimates (Z_1) from the PSDM data and the stratigraphic framework based on the deformation structures at the BCU ($Z_1 = Z_{Moho} - Z_{BCU}$). Various Moho depth estimates (regional grid or the PSDM velocity model) using initial crustal thicknesses (Z_0) of 30 to 35 km were used. The results ($\beta = Z_0/Z_1$) are plotted above the three regional profiles in Figures 5–7. On the N–S profile, β increases from >1 in the north to 8.7 in the South Porcupine Basin, then decreasing to <3 toward the northeastern part of the Western Approaches Margin (Figure 5). The observation is consistent with the estimate of *Tate et al.* [1993] of β being lower under the PMVR but significantly higher in the South Porcupine Basin. The east–west oriented profile 11240 (Figure 7) shows values consistent with a stretching peak of $\beta > 3.5$ in the center of the basin. The profile 11200–11220 (Figure 6) shows a lower estimate of $\beta > 4.6$ compared to the $\beta = 5.7$ peak below the PMVR.

5.3. PMVR Volume and Life Span

[23] The potential life span of the PMVR can be evaluated by estimating its melt volume and melt production rates [*White et al.*, 2006]. The mean thickness of the ridge is about 2 km, with a maximum observed thickness of 5.2 km (Figures 8b and 9a). The length of the main body of the PMVR (N–S axis) is estimated to range from 85 to >95 km, while the width is about 17 to 25 km. The volume of the PMVR can be estimated assuming a triangular prism shape with a basal surface of 17 km^2 to 25 km^2, and an average thickness of 2 km to 5.2 km. Using these values, the volume of the ridge is between 1445 km^3 and 5850 km^3. The life span of the PMVR was calculated from the obtained volumes using the production rates (Qe) for various geological settings (oceanic Qe min: 0,023 km^3/y, Qe max: 0,033 km^3/y; continental crust Qe min: 0,004 km^3/y, Qe max: 0,005 km^3/y; continental flood basalt Qe min: 0.7 km^3/y, Qe max: 0.11 km^3/y [*White et al.*, 2006] (Figure 11)). For the different settings, the volume of the PMVR represents an emplacement duration of 44 ky to 254 ky (oceanic), 278 ky to 1.625 My (continental crust), 2 ky to 53 ky (continental flood basalt). The obtained estimates are the minimum durations, as the thermal relaxation and the potential hiatuses between eruptions of melt to the surface are ignored.

[24] To our knowledge the only calibrated analogous volcanic feature that has been constrained in terms of geometry/volume and duration crops out in the Nuusuaq Basin of West Greenland [*Pedersen et al.*, 2002]. The minimum estimated production rate of 0.042 km^3/y for this hyaloclastite outcrop is approaching the values of the oceanic setting of

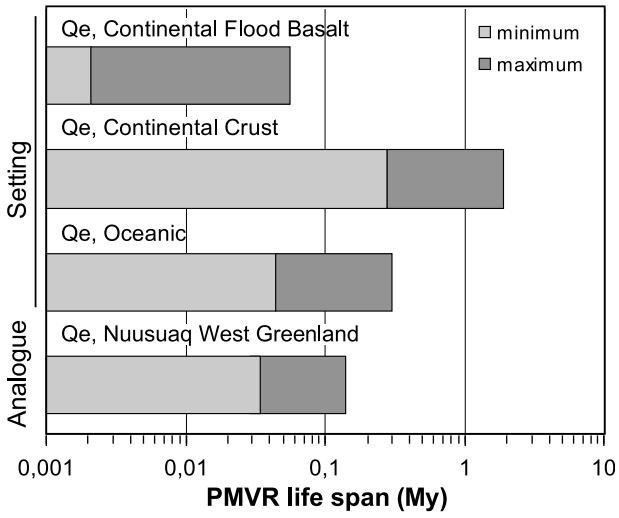

Figure 11. Various life span estimations for the PMVR from the production rates of volcanism in three different settings. Production rates used were compiled by *White et al.* [2006].

White et al. [2006]. Using the *Pedersen et al.* [2002] production rate for the PMVR, the potential life span of the ridge is 34 to 140 ky.

5.4. Thermomechanical Modeling of the Porcupine Basin

[25] Interpretation of the seismic data shows that magmatic features are present within the Porcupine crust and the basin floor. In order to support the seismic interpretations, we proceed to demonstrate that, based on the crustal extension and the life span of the rifting, the thermomechanical requisites for melt production and magmatism exist within the basin.

[26] With a volcanic ridge thickness of 2 to 5.2 km, assuming that the ridge represents the entire melt thickness (i.e., assuming no thickening of the lower crust), the potential mantle temperature for stretching factors of 2 to 5 ranges from ~1350–1450°C to 1290–1350°C, respectively (PMVR, orange area in Figure 12a). Considering the estimates of the minimum stretching factors in the vicinity of the PMVR (β = 2.6–4.5, Figure 3b), the potential melt temperature (1400°C) required to produce the PMVR thickness corresponds to a rifting event of maximum of 13.5 Myr (green area PMVR βc in Figure 12b). Taking the estimate of a stretching factor of β = 3.7–6 near the PMVR by *Tate et al.* [1993] and considering two potential mantle temperatures (yellow area for 1350°C and pink area for 1400°C in Figure 12b), the associated rifting

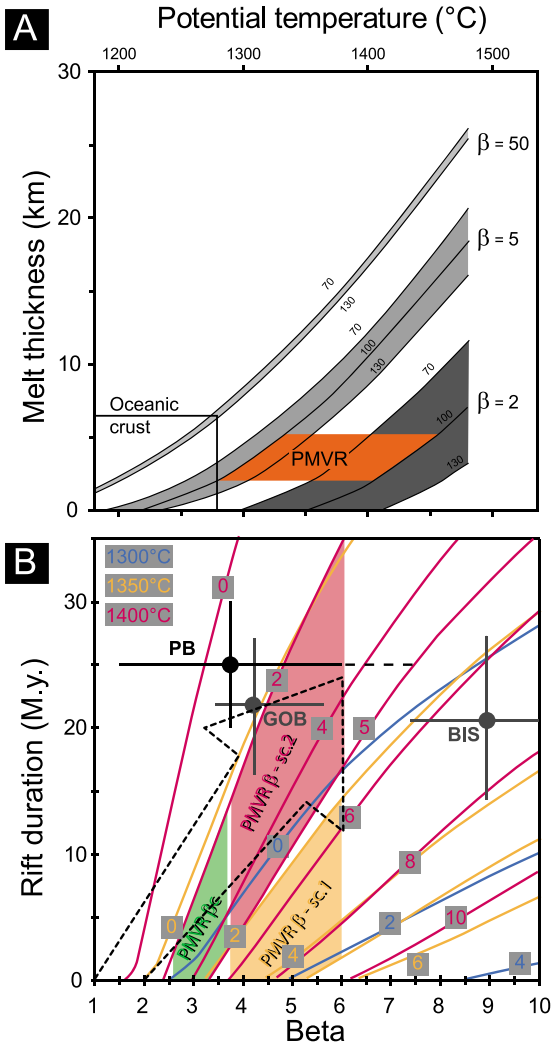

Figure 12. Thermomechanical properties of the Porcupine Basin and the PMVR. (a) Predictive melt thicknesses generated by adiabatic decompression of asthenospheric mantle for various potential temperatures [*McKenzie and Bickle*, 1988]. The domain of the potential melt thickness within the PMVR corresponding to melt temperatures of 1290–1450°C, a plate thickness of 118 km, and a stretching factor of 2 to 5, is highlighted in orange (see text for more detailed description). (b) The control of the stretching factor (β) during rifting and the rift duration on melt production, assuming an initially thermally relaxed lithosphere (colored lines after *Bown and White* [1995]). Note that the duration of the main rifting event is updated to better reflect the published duration spans of 20–30 Myr (Figure 2). Taking the corrected life span and the temporal evolution of the β into account, it is clear that the field of synrift partial melting is reached in the Porcupine Basin. Furthermore, the inferred lower limit of the extension (β = 2.25–3.5) of the melting field coincides closely with the observed northern extent of the PMVR (Figure 3c). See text for further discussion.

duration is, respectively, 3–35 Myr (PMVR β – sc1 in Figure 12b) and instantaneous to 14.5 My (PMVR β – sc2 in Figure 11b).

[27] The duration of the main rifting period during the Late Jurassic – Early Cretaceous has been constrained to maximum 20–30 Myr [e.g., *Tate et al.*, 1993] (Figure 2). In this context it is worth noting that there has been some confusion about the duration of the main rifting event, possibly because *Tate et al.* [1993] suggest that the rifting started near the base of the Bajocian, the age of which was in 1993 defined as c. 180 Ma, and lasted until the end of the Tithonian, defining a rift duration of 35–40 Ma. However, the base of the Bajocian has been redefined to c. 171–172 Ma and the top Tithonian to 145–146 Ma [e.g., *Gradstein et al.*, 2004; International Stratigraphic Chart, International Commission on Stratigraphy, 2004], giving a revised rifting duration of c. 25–27 Myr for the interpretation of *Tate et al.* [1993]. A rifting duration in the order of 15–25 Myr for the Porcupine Basin has also been indicated independently by several other authors (Figure 2). The difference of 10–20 Myr in the rifting duration has significant implications for the thermomechanical evolution of the basin (Figure 12b); cf. *Reston et al.* [2004] where the conclusion of the absence of magmatism in the basin is largely relying on a rift duration of c. 40 Myr). The results confirm that the duration of the main rifting event is likely to be significantly less than 40 Myr.

[28] In addition to the rifting duration, the development of the stretching factor (β) through time needs to be taken into account (turquoise arrow in Figure 12b). As the Porcupine Basin experienced minor rifting before the main rifting event [e.g., *Tate et al.*, 1993], an initial, modest stretching factor of 1.5 is assumed. A rift duration of 20–30 Myr plotted against β, with the temporal evolution of β taken into account (β changing from 1.5 to 6; the dashed black arrow in Figure 12b), shows that the partial melt field was reached in the Porcupine Basin during the main rifting.

[29] There is no conflict between the observed rifting period and the late- to post-rift timing of the igneous activity. Among others, *Keen et al.* [1994] demonstrate that a considerable delay between the onset of rifting and the onset of magmatism may occur and is a natural consequence of decompressional mantle melting. Heat flow modeling of the Porcupine Basin by *Baxter et al.* [2001] shows a delay of 30 Myr between the rifting and the maximum basement heat flow. In contrast, we argue that post-rift serpentinite mud volcanism was inhibited by the removal of its thermomechanical prerequisites, i.e., the tectonic quiescence together with thermal relaxation reversing the embrittlement of the lower and middle crust and leading to a cessation of water transport into the lower crust/upper mantle.

5.5. Rift Basins With Intrabasement Highs

[30] The observations indicate that the PMVR is a volcanically derived hyaloclastic mound, analogous to the mounds observed in the subsurface of the West Indian Volcanic Margin (the Somnath Ridge (Figure 8d) [*Calvès et al.*, 2008, 2011]) or the Eastern Continental Margin of India at the northern tip of the 85°E Ridge within the Mahanadi offshore basin [*Subrahmanyam et al.*, 2008; *Bastia et al.*, 2010]. Both volcanic mounds are capped by extensive shallow water carbonate platforms (above mound M2 in the PMVR). The carbonate platform of the PMVR can be used as a paleo-bathymetric marker of near-sea level in the Porcupine Basin. This observation ties with the flexural forward modeling of *Baxter et al.* [2001]. The potential analogy of the hyaloclastic mounds with other equivalent edifices observed in Faroe Escarpment [*Kiørboe*, 1999] and other volcanic provinces [*Planke et al.*, 1999, 2000] allows us to attribute a potential tholeïtic basaltic origin to the PMVR. This type of intrabasement high within rifted margins represents the focus of magmatism during the early stages of passive margin evolution.

5.6. Geodynamic Position of the PMVR

[31] In the case of the Porcupine Basin, the PMVR represents the expression of a regional magmatic pulse of early Cretaceous age. Within the nearby rifted Rockall Trough, the Barra Volcanic Ridge System (BVRS) has been identified as representing an early Cretaceous volcanic pulse [*Scrutton and Bentley*, 1988]. This ridge system is located on the northern side of the Charie-Gibbs fracture zone, whereas the PMVR is located south of the proposed linked Clare lineament [*Tate*, 1992]. In the framework of the opening of the North Atlantic, magmatic events (J anomaly, aged ~130–125 Ma) along the Newfoundland-Galicia conjugate margins may predate the oceanization [*Bronner et al.*, 2011], the Porcupine Basin may represent a northern expression of the magmatic pulse recorded by the J anomaly (Figure 1). Further north along the Norwegian continental margin, volcanic seamounts have been described by *Lundin and Doré* [1997] in the southern Vøring Basin. The timing of rifting in

the Porcupine and the magmatism, and the position of the basin with respect to the known plate organization at early Cretaceous time suggests a close relationship between the events. All together, these volcanic features PMVR and BVRS delineate zone as wide as 200 km north of the identified continent ocean boundary between Eurasia and North America during the early Cretaceous. This associated with the J Anomaly extension, could led to the identification of relatively small magmatic province extending from the Newfoundland fracture zone, extending northward through the Porcupine Basin, and ending toward the NW in the southern part of the Rockall Trough spanning a distance of 1700 km. This scheme could lead to understand the organization of the plate setting in the propagating phases of the opening of the North Atlantic.

6. Conclusions

[32] The Porcupine Median Ridge represents a hyaloclastic mound extruded and deposited close to sea level, similarly to other margins such as the Faroe-Shetland Basin and the East and West Indian margins. The new seismic images presented herein conclusively rule out previously proposed origins of the Median Ridge as linked to serpentinite mud volcanism and rotated fault blocks.

[33] The conclusion is supported by several observations, most importantly: (1) the architecture of the ridge in the seismic reflection data, showing a volcanic sequence with progradational hyaloclastite deltas and a carbonate platform; (2) the architecture of the crust, showing a crustal detachment offset by late, steep, crustal-scale faults; (3) the seismic velocity structure of the ridge and the crust, showing relatively low seismic velocities typical for basalt and hyaloclastic material rather than for extensively serpentinized mantle or serpentinite mud; (4) the presence of a gravity anomaly beneath the Porcupine Arch and the associated high seismic velocity gradient, indicating a presence of melts in the lower crust; (5) the age of the ridge, indicating that it formed after the cessation of the main rifting, thus removing the mechanical prerequisites for mantle serpentinization and serpentinite mud volcanism; (6) the association of early Cretaceous magmatic features observed in the Newfoundland-Galicia margins, the Porcupine Basin, the Rockall Basin and the Vøring Basin, which could lead to the identification of a patched large igneous province in the North Atlantic; and (7) the subaerial volcanic origin and presence of a carbonate platform provide an important calibration of the subsidence history and should have important implications for hydrocarbon prospectivity of the Porcupine Basin.

Acknowledgments

[34] This study has been largely inspired by the IONGXT NE Atlantic SPAN survey and ION-GXT is gratefully acknowledged for giving us access to the data. G.C. carried this work during an English summer in Manchester University–School of Earth, Atmospheric and Environmental Sciences as research visitor. T.T. was supported by the Virtual Seismic Atlas project (www.seismicatlas.org). SMT (now IHS) Kingdom is thanked for their Software University Grant, which allowed this work to take place. We are grateful for reviews from Joe Cartwright and Sverre Planke, the Associate Editor Robert Dunn, and the Editor James Tyburczy, all of whom helped to improve the paper.

References

Bastia, R., M. Radhakrishna, S. Das, A. S. Kale, and O. Catuneanu (2010), Delineation of the 85°E ridge and its structure in the Mahanadi Offshore Basin, Eastern Continental Margin of India (ECMI), from seismic reflection imaging, *Mar. Pet. Geol.*, *27*(9), 1841–1848, doi:10.1016/j.marpetgeo.2010.08.003.

Baxter, K., T. Buddin, D. V. Corcoran, and S. Smith (2001), Structural modelling of the south Porcupine Basin, offshore Ireland: Implications for the timing, magnitude and style of crustal extension, *Geol. Soc. Spec. Publ.*, *188*, 275–290, doi:10.1144/GSL.SP.2001.188.01.16.

Bentley, P. A. D., and R. A. Scrutton (1987), Seismic investigation into the structure of southern Rockall Trough, in *Petroleum Geology of North West Europe*, edited by J. Brooks and K. W. Glennie, pp. 67–75, Graham and Trotman, London.

Berndt, C., S. Planke, E. Alvestad, F. Tsikalas, and T. Rasmussen (2001), Seismic volcanostratigraphy of the Norwegian Margin: Constraints on tectonomagmatic break-up processes, *J. Geol. Soc.*, *158*(3), 413–426, doi:10.1144/jgs.158.3.413.

Boillot, G., S. Grimaud, A. Mauffret, D. Mougenot, J. Kornprobst, J. Mergoil-Daniel, and G. Torrent (1980), Ocean-continent boundary off the Iberian margin: A serpentinite diapir west of the Galicia Bank, *Earth Planet. Sci. Lett.*, *48*(1), 23–34, doi:10.1016/0012-821X(80)90166-1.

Bown, J. W., and R. S. White (1995), Effect of finite extension rate on melt generation at rifted continental margins, *J. Geophys. Res.*, *100*(B9), 18,011–18,029, doi:10.1029/94JB01478.

British Oceanographic Data Centre (2003), GEBCO Digital Atlas, Centenary Edition [CD-ROM], Liverpool, U. K.

Bronner, A., D. Sauter, G. Manatschal, G. Péron-Pinvidic, and M. Munschy (2011), Magmatic breakup as an explanation for magnetic anomalies at magma-poor rifted margins, *Nat. Geosci.*, *4*, 549–553, doi:10.1038/ngeo1201.

Calvès, G., P. D. Clift, and A. Inam (2008), Anomalous subsidence on the rifted volcanic margin of Pakistan: No influence from Deccan plume, *Earth Planet. Sci. Lett.*, *272*(1–2), 231–239, doi:10.1016/j.epsl.2008.04.042.

Calvès, G., A. M. Schwab, M. Huuse, P. D. Clift, C. Gaina, D. Jolley, A. R. Tabrez, and A. Inam (2011), Seismic volcanostratigraphy of the western Indian rifted margin: The pre-Deccan igneous province, *J. Geophys. Res.*, *116*, B01101, doi:10.1029/2010JB000862.

Conroy, J. J., and A. Brock (1989), Gravity and magnetic studies of crustal structure across the Porcupine basin west of Ireland, *Earth Planet. Sci. Lett.*, *93*(3–4), 371–376, doi:10.1016/0012-821X(89)90036-8.

Corti, G., M. Bonini, S. Conticelli, F. Innocenti, P. Manetti, and D. Sokoutis (2003), Analogue modelling of continental extension: A review focused on the relations between the patterns of deformation and the presence of magma, *Earth Sci. Rev.*, *63*(3–4), 169–247, doi:10.1016/S0012-8252(03)00035-7.

Courtier, A. M., D. J. Hart, and N. I. Christensen (2004), Seismic properties of Leg 195 serpentinites and their geophysical implications, *Proc. Ocean Drill. Program Sci. Results*, *195*, 1–12.

Deregowski, S. M. (1990), Common-offset migrations and velocity analysis, *First Break*, *8*, 225–234.

Doré, A. G., E. R. Lundin, L. N. Jensen, Ø. Birkeland, P. E. Eliassen, and C. Fichler (1999), Principal tectonic events in the evolution of the northwest European Atlantic margin, in *Petroleum Geology of Northwest Europe: Proceedings of the 5th Conference*, *Pet. Geol. Conf. Ser.*, vol. 5, edited by A. J. Fleet and S. A. R. Boldy, pp. 41–61, Geol. Soc., London, doi:10.1144/0050041.

Emery, D., and K. J. Myers (1996), *Sequence Stratigraphy*, 297 pp., Blackwell Sci., Oxford, U. K., doi:10.1002/9781444313710.

Grad, M., T. Tiira, and the ESC Working Group (2009), The Moho depth map of the European Plate, *Geophys. J. Int.*, *176*, 279–292, doi:10.1111/j.1365-246X.2008.03919.x.

Gradstein, F. M., J. G. Ogg, A. G. Smith, W. Bleeker, and L. J. Lourens (2004), A new geologic time scale, with special reference to Precambrian and Neogene, *Episodes*, *27*(2), 83–100.

Hall, B. D., and N. White (1994), Origin of anomalous Tertiary subsidence adjacent to North Atlantic continental margins, *Mar. Pet. Geol.*, *11*(6), 702–714, doi:10.1016/0264-8172(94)90024-8.

Johnson, H., J. D. Ritchie, R. W. Gatliff, J. P. Williamson, J. Cavill, and J. Bulat (2001), Aspects of the structure of the Porcupine and Porcupine Seabight basins as revealed from gravity modelling of regional seismic transects, *Geol. Soc. Spec. Publ.*, *188*, 265–274, doi:10.1144/GSL.SP.2001.188.01.15.

Johnston, S., A. G. Doré, and A. M. Spencer (2001), The Mesozoic evolution of the southern North Atlantic region and its relationship to basin development in the south Porcupine Basin, offshore Ireland, *Geol. Soc. Spec. Publ.*, *188*, 237–263, doi:10.1144/GSL.SP.2001.188.01.14.

Jones, G., L. S. Williams, and R. J. Knipe (2004), Structural evolution of a complex 3D fault array in the Cretaceous and Tertiary of the Porcupine Basin, offshore Ireland, *Mem. Geol. Soc.*, *29*, 117–132.

Jones, S. M., N. White, and B. Lovell (2001), Cenozoic and Cretaceous transient uplift in the Porcupine Basin and its relationship to a mantle plume, in *The Petroleum Exploration of Ireland's Offshore Basins*, edited by P. M. Shannon, P. D. W. Haughton, and D. V. Corcoran, *Geol. Soc. Spec. Publ.*, *188*, 345–360, doi:10.1144/GSL.SP.2001.188.01.20.

Keen, C. E., R. C. Courtney, S. A. Dehler, and M.-C. Williamson (1994), Decompression melting at rifted margins: Comparison of model predictions with the distribution of igneous rocks on the eastern Canadian margin, *Earth Planet. Sci. Lett.*, *121*(3–4), 403–416, doi:10.1016/0012-821X(94)90080-9.

Kiørboe, L. (1999), Stratigraphic relationships of the Lower Tertiary of the Faeroe Basalt Plateau and the Faeroe–Shetland Basin, in *Petroleum Geology of Northwest Europe: Proceedings of the 5th Conference*, edited by A. Fleet and S. A. R. Boldy, pp. 559–579, Geol. Soc., London.

Lundin, E. R., and A. G. Doré (1997), A tectonic model for the Norwegian passive margin with implications for the NE Atlantic: Early Cretaceous to break-up, *J. Geol. Soc.*, *154*, 545–550, doi:10.1144/gsjgs.154.3.0545.

Masson, D. G., and P. R. Miles (1986), Structure and development of Porcupine Seabight sedimentary basin, offshore southwest Ireland, *AAPG Bull.*, *70*(5), 536–548.

Masson, F., A. W. B. Jacob, C. Prodehl, P. W. Readman, P. M. Shannon, A. Schulze, and U. Enderle (1998), A wide-angle seismic traverse through the Variscan of southwest Ireland, *Geophys. J. Int.*, *134*(3), 689–705, doi:10.1046/j.1365-246x.1998.00572.x.

McCann, T., P. M. Shannon, and J. G. Moore (1995), Fault patterns in the cretaceous and tertiary (end syn-rift, thermal subsidence) succession of the Porcupine Basin, offshore Ireland, *J. Struct. Geol.*, *17*(2), 201–214, doi:10.1016/0191-8141(94)E0037-Y.

McKenzie, D., and M. J. Bickle (1988), The volume and composition of melt generated by extension of the lithosphere, *J. Petrol.*, *29*(3), 625–679, doi:10.1093/petrology/29.3.625.

Mitchum, R. M., P. R. Vail, and J. B. Sangree (1977), Stratigraphic interpretation of seismic reflection patterns in depositional sequences, part 6, in *Seismic Stratigraphy: Application to Hydrocarbon Exploration*, 8th ed., edited by C. E. Payton, pp. 117–133, Am. Assoc. of Pet. Geol., Tulsa, Okla.

Moore, J. G., and P. M. Shannon (1995), The Cretaceous succession in the Porcupine Basin, offshore Ireland: Facies distribution and hydrocarbon potential, *Geol. Soc. Spec. Publ.*, *93*, 345–370, doi:10.1144/GSL.SP.1995.093.01.28.

O'Reilly, B. M., F. Hauser, C. Ravaut, P. M. Shannon, and P. W. Readman (2006), Crustal thinning, mantle exhumation and serpentinization in the Porcupine Basin, offshore Ireland: Evidence from wide-angle seismic data, *J. Geol. Soc.*, *163*, 775–787, doi:10.1144/0016-76492005-079.

O'Sullivan, J. M., S. M. Jones, and R. J. Hardy (2010a), Geological modelling of the Porcupine Median Ridge: Implications for the hydrocarbon prospectivity of North Atlantic hyper-extensional basin and margin systems, *Search Disc. Art., 10253*, Am. Assoc. of Pet. Geol., Tulsa, Okla.

O'Sullivan, J. M., S. M. Jones, and R. J. Hardy (2010b), Comparative analysis of the Porcupine Median Volcanic Ridge with modern day Pacific Ocean seamounts—Further evidence of an amagmatic Mesozoic basin history for the South Porcupine Basin, offshore Ireland, paper presented at II Central and North Atlantic Conjugate Margins Conference, Univ. of Lisboa, Lisbon.

Pedersen, A. K., L. M. Larsen, P. Riisager, and K. S. Dueholm (2002), Rates of volcanic deposition, facies changes and movements in a dynamic basin: The Nuussuaq Basin, West Greenland, around the C27n-C26r transition, in *The North Atlantic Igneous Province: Stratigraphy, Tectonic, Volcanic and Magmatic Processes*, edited by D. W. Jolley and B. R. Bell, *Geol. Soc. Spec. Publ.*, *197*, 157–181, doi:10.1144/GSL.SP.2002.197.01.07.

Peron-Pinvidic, G., and G. Manatschal (2010), From microcontinents to extensional allochthons; witnesses of how continents rift and break apart? (in Stretching the crust and extending exploration frontiers), *Pet. Geosci.*, *16*(3), 189–197, doi:10.1144/1354-079309-903.

Planke, S., E. Alvestad, and O. Eldholm (1999), Seismic characteristics of basaltic extrusive and intrusive rocks, *Leading Edge*, *18*, 342–348, doi:10.1190/1.1438289.

Planke, S., P. A. Symonds, E. Alvestad, and J. Skogseid (2000), Seismic volcanostratigraphy of large-volume basaltic extrusive complexes on rifted margins, *J. Geophys. Res.*, *105*(B8), 19,335–19,351, doi:10.1029/1999JB900005.

Ranero, C. R., and M. Pérez-Gussinyé (2010), Sequential faulting explains the asymmetry and extension discrepancy of conjugate margins, *Nature*, *468*, 294–299, doi:10.1038/nature09520.

Readman, P. W., B. M. O'Reilly, P. M. Shannon, and D. Naylor (2005), The deep structure of the Porcupine Basin, offshore Ireland, from gravity and magnetic studies, in *Petroleum Geology: North–West Europe and Global Perspectives—Proceedings of the 6th Petroleum Geology Conference*, *Pet. Geol. Conf. Ser.*, vol. 6, pp. 1047–1056, Geol. Soc., London, doi:10.1144/0061047.

Reston, T. J., J. Pennell, A. Stubenrauch, I. Walker, and M. Perez-Gussinye (2001), Detachment faulting, mantle serpentinization, and serpentinite-mud volcanism beneath the Porcupine Basin, southwest of Ireland, *Geology*, *29*, 587–590, doi:10.1130/0091-7613(2001)029<0587:DFMSAS>2.0.CO;2.

Reston, T. J., V. Gaw, J. Pennell, D. Klaeschen, A. Stubenrauch, and I. Walker (2004), Extreme crustal thinning in the south Porcupine Basin and the nature of the Porcupine Median High: Implications for the formation of non-volcanic rifted margins, *J. Geol. Soc.*, *161*, 783–798, doi:10.1144/0016-764903-036.

Rey, S. S., S. Planke, P. A. Symonds, and J. I. Faleide (2008), Seismic volcanostratigraphy of the Gascoyne margin, Western Australia, *J. Volcanol. Geotherm. Res.*, *172*(1–2), 112–131, doi:10.1016/j.jvolgeores.2006.11.013.

Sandwell, D. T., and W. H. F. Smith (2009), Global marine gravity from retracked Geosat and ERS-1 altimetry: Ridge Segmentation versus spreading rate, *J. Geophys. Res.*, *114*, B01411, doi:10.1029/2008JB006008.

Scrutton, R. A., and P. A. D. Bentley (1988), Major Cretaceous volcanic province in southern Rockall Trough, *Earth Planet. Sci. Lett.*, *91*(1–2), 198–204, doi:10.1016/0012-821X(88)90161-6.

Shannon, P. M. (1991), The development of Irish offshore sedimentary basins, *J. Geol. Soc.*, *148*, 181–189, doi:10.1144/gsjgs.148.1.0181.

Sibuet, J.-C., S. Srivastava, and G. Manatschal (2007), Exhumed mantle-forming transitional crust in the Newfoundland-Iberia rift and associated magnetic anomalies, *J. Geophys. Res.*, *112*, B06105, doi:10.1029/2005JB003856.

Sinclair, K., P. M. Shannon, B. P. J. Williams, S. D. Harker, and J. G. Mooren (1994), Tectonic control on sedimentary evolution of three North Atlantic borderland Mesozoic basins, *Basin Res.*, *6*(4), 193–217, doi:10.1111/j.1365-2117.1994.tb00085.x.

Srivastava, S. P., J.-C. Sibuet, S. Cande, W. R. Roest, and I. D. Reid (2000), Magnetic evidence for slow seafloor spreading during the formation of the Newfoundland and Iberian margins, *Earth Planet. Sci. Lett.*, *182*(1), 61–76, doi:10.1016/S0012-821X(00)00231-4.

Subrahmanyam, V., A. S. Subrahmanyam, G. P. S. Murty, and K. S. R. Murthy (2008), Morphology and tectonics of Mahanadi Basin, northeastern continental margin of India from geophysical studies, *Mar. Geol.*, *253*(1–2), 63–72, doi:10.1016/j.margeo.2008.04.007.

Sullivan, K. D. (1983), The Newfoundland Basin: Ocean-continent boundary and Mesozoic seafloor spreading history, *Earth Planet. Sci. Lett.*, *62*(3), 321–339, doi:10.1016/0012-821X(83)90003-1.

Symonds, P. A., S. Planke, O. Frey, and J. Skogseid (1998), Volcanic evolution of the Western Australian continental margin and its implications for basin development, in *The Sedimentary Basins of Western Australia*, vol. 2, edited by P. G. Purcell and R. R. Purcell, pp. 33–54, Pet. Explor. Soc. of Aust., Perth, West. Aust.

Tate, M. P. (1992), The Clare Lineament: A relic transform fault west of Ireland, in *Basins on the Atlantic Seaboard: Petroleum Geology, Sedimentology and Basin Evolution*, edited by J. Parnell, *Geol. Soc. Spec. Publ.*, *62*, 375–384, doi:10.1144/GSL.SP.1992.062.01.28.

Tate, M. P. (1993), Structural framework and tectono-stratigraphic evolution of the Porcupine Seabight Basin, offshore Western Ireland, *Mar. Pet. Geol.*, *10*(2), 95–123, doi:10.1016/0264-8172(93)90016-L.

Tate, M. P., and M. R. Dobson (1988), Syn- and post-rift igneous activity in the Porcupine Seabight Basin and adjacent continental margin W of Ireland, in *Early Tertiary Volcanism and the Opening of the NE Atlantic*, edited by A. C. Morton and L. M. Parson, *Geol. Soc. Spec. Publ.*, *39*, 309–334, doi:10.1144/GSL.SP.1988.039.01.28.

Tate, M. P., and M. R. Dobson (1989), Late Permian to early Mesozoic rifting and sedimentation offshore NW Ireland, *Mar. Pet. Geol.*, *6*(1), 49–59, doi:10.1016/0264-8172(89)90075-5.

Tate, M., N. White, and J.-J. Conroy (1993), Lithospheric Extension and Magmatism in the Porcupine Basin West of Ireland, *J. Geophys. Res.*, *98*(B8), 13,905–13,923.

White, N., M. Tate, and J.-J. Conroy (1992), Lithospheric stretching in the Porcupine Basin west of Ireland, in *Basins on the Atlantic Seaboard: Petroleum Geology, Sedimentology and Basin Evolution*, edited by J. Parnell, *Geol. Soc. Spec. Publ.*, *62*, 327–331, doi:10.1144/GSL.SP.1992.062.01.25.

White, S. M., J. A. Crisp, and F. J. Spera (2006), Long-term volumetric eruption rates and magma budgets, *Geochem. Geophys. Geosyst.*, *7*, Q03010, doi:10.1029/2005GC001002.

Williams, B. P. J., P. M. Shannon, and I. K. Sinclair (1999), Comparative Jurassic and Cretaceous tectono-stratigraphy and reservoir development in the Jeanne d'Arc and Porcupine Basins, in *Petroleum Geology of Northwest Europe: Proceedings of the 5th Conference*, edited by A. J. Fleet and S. A. R. Boldy, pp. 487–499, Geol. Soc., London.

Ziegler, P. A. (1988), *Evolution of the Arctic North Atlantic and the Western Tethys*, *AAPG Mem.*, *43*, 198 pp.